Executive Summary

Major results on Tasks 1-4 under the Memorandum of Understanding for the period June 1 2004 – May 31 2005 can be summarized as follows:

Task 1: Range Correction Algorithm/Convective Stratiform Separation Algorithm: As documented in the Interim Report, work is ongoing to demonstrate the value of range correction of radar rainfall observations in hydrologic modeling. For a set of cases within the State College Pennsylvania WSR-88D umbrella in which radar-only estimates were compared with gauge-radar multisensor estimates, range correction increased the correlation between the radar-only and multisensor fields. Previous work has shown that the multisensor estimates produced the best streamflow simulations within the Hydrology Laboratory's research distributed hydrologic model. Therefore we are confident that we can demonstrate that range correction leads to improved streamflow forecasts when the precipitation input to the hydrologic model is based only on radar.

Staff in OHD have begun preparation of a journal article on the Convective-Stratiform Separation Algorithm, including an evaluation of its role in improving the results of the Range Correction Algorithm.

Task 2. Effects of increased resolution on radar rainfall estimates: Work performed by Princeton University under the OHD collaborative agreement showed that increasing the spatial resolution of radar rainfall estimates can increase their accuracy relative to rain gauge observations, provided that temporal resolution of the radar estimates is also higher. It is apparent from coincident radar and disdrometer estimates of reflectivity that radar can detect small-scale rainfall features, but that some precision is lost if temporal sampling frequency is only 4-6 minutes, as it is with current volume coverage patterns.

Task 3. Probabilistic Quantitative Precipitation Estimates: Work performed both under contract by the University of Iowa and validated by OHD has shown that the error distribution for radar rainfall estimates can be described simply by a set of power-law functions requiring between 4 and 6 parameters in total. We infer that it might be possible to correct the current horizontal-polarization algorithm rainfall for magnitude-dependent biases using one of these power-law relations. Furthermore, it appears that the statistical model for rainrate-dependent bias might be applied to reducing RMS errors for heavier rainfall amounts.

Task 4: Evaluation of dual-polarization radar precipitation estimates: A preliminary study in the Interim Report showed that within a limited set of cases from the 2004 warm season, the KOUN dual-polarization "synthetic" algorithm had a higher correlation and lower RMS error relative to 1-h gauge reports than did coincident observations from the KTLX WSR-88D. There still appear to be rainrate-dependent biases in the dual-polarization estimates, similar to those in the operational Digital Precipitation Array product. This work is now being extended with data from 2005 and reprocessed cases from 2004.

Office of Hydrologic Development staff have also undertaken additional work to assist the Radar Operations Center Applications Branch in analyzing results from proposed

modifications to the Radar Echo Classifier (REC) algorithm, and to organize routine teleconferences with the National Severe Storms Laboratory to discuss results of our Independent Validation and Verification of dual-polarization rainfall estimation algorithms.

Task 1: Validate and Enhance Vertical Profile of Reflectivity-Range Correction Algorithms and Convective-Stratiform Separation Algorithm

Following the recommendation of the NEXRAD Technical Advisory Committee that we demonstrate the benefit of the RCA-CSSA package to hydrologic modeling, we have prepared a dataset of radar estimates for input to the Hydrology Laboratory-Modeling System (HL-RMS), a distributed hydrologic modeling system. Data are from the period October 2002-January 2003, in the State College PA (KCCX) umbrella.

Initial results for the Juniata Basin, which lies entirely within the KCCX 230-km umbrella, indicate that the radar estimates both with and without range correction produce a realistic hydrologic response. However, both sets of estimates are seriously biased, and we will apply a mean-field bias correction with coincident gauge data before proceeding further. Though a dense rain gauge network exists in this area, we will use the information only for mean-field bias. No spatial detail will be contributed by the rain gauge data.

Also, since the Juniata basin lies very close to the RDA, it is not an ideal test area when considered in isolation, since it is within the zone generally not affected seriously by range effects. The Juniata was selected because it contains several unregulated headwater basins with long stream gauge records, and it has been studied thoroughly by HL in the past. We are now identifying other test basins within the KCCX umbrella to demonstrate effects of range correction on precipitation estimates over a substantial portion of the radar umbrella.

We will note that over the KCCX umbrella as a whole, the RCA-CSSA corrections have produced significant improvements in precipitation estimates as validated by Multisensor Precipitation Estimator (MPE) fields, which are based on a radar mosaic and coincident gauge data. For one event in January 2003, which resulted in 25-mm rainfall over most of the umbrella and produced a significant rise on the Juniata and other rivers, range correction reduced the RMS difference between KCCX estimates and the multisensor estimates from 16.9 mm to 10.4 mm. Range correction also reduced the gauge/radar bias from 1.14 to 1.04. These figures are for the basin as a whole.

Delays in processing the level II data for the KCCX umbrella prevented a complete set of HL-RMS runs for more basins within the KCCX umbrella at the time of writing. However, for the period October 2002 through January 2003 we have a complete set of radar precipitation estimates, with and without range correction, for all events known to have produced a rise in the Juniata River.

Following receipt of information from the ROC Applications Branch that the RCA/CSSA package took up substantial CPU time, compared to the rest of the Precipitation Processing System, we analyzed CPU usage among various components of the two algorithms. For four cases (KCCX_01/01/03; KCCX_101602; KEAX_032304; KLWX_032305), the numbers were typically as follows:

- CSSA TEXTURE_R ranged from ~1.25 to 3.25 sec (reflectivity texture calculation)

- RCA MVPR ranged from 0.15 to 1.25 sec (mean vertical profile of reflectivity calculation)
- Rest of processing was about 1.0 sec.

In most cases, TEXTURE_R was decidedly predominant (4.21 sec of a total of 5.23 sec in the KCCX_101602 case, for example). Subject to continuation of the project, we therefore plan to examine the CSSA algorithm for potential economies, such as calculating texture only in areas with some minimal reflectivity, and possibly not at every azimuth-range point.

Though operational implementation of the RCA-CSSA package within the ORPG has been deferred on the advice of the NEXRAD Technical Advisory committee, we have investigated the possibility of implementing a version of the RCA algorithm within AWIPS, relying on volumetric reflectivity data available there. Initial results are encouraging in that, even with this rather limited data, it is possible to derive vertical profiles of reflectivity with the same basic pattern and features as those derived from full volumetric base reflectivity. Also, a form of range correction is envisioned for precipitation products derived from the national-scale radar reflectivity mosaic currently under development by NSSL, NCEP, and OHD.

Task 2: Assessment of Increased Resolution of Reflectivity Estimates On Precipitation Estimates

Data from the Terminal Doppler Weather Radar (TDWR) system maintained by the Federal Aviation Administration are potentially very valuable for NWS warning operations, since their siting often provides better surveillance of metropolitan areas than can the nearest WSR-88D unit. The possibilities for flash flood detection are particularly intriguing in that the TDWR features higher spatial resolution than has the WSR-88D to date (300 m x 1° vs. 1000 m x 1°), and scanning patterns that permit 1-minute updates of 0.5° PPI fields. The advantages are partially offset by the TDWR's C-band electronics, which makes observations in heavy rainfall subject to attenuation.

As noted in the MOU, we extended a collaborative agreement with the Princeton University Department of Civil and Environmental Engineering (principal investigator James. A. Smith) to include a comparison of rainfall estimates from the current WSR-88D at Sterling, VA (KLWX) with estimates derived from low-elevation reflectivity observations from the TDWR unit for Baltimore-Washington International Airport (referred to as TBWI). The study is designed to show the effects of proposed enhancements to the spatial resolution of WSR-88D reflectivity fields, and to demonstrate possible methods of mosaicking TDWR and WSR-88D estimates. Hereafter, we refer to the report on its results (Smith and Baeck 2005) as SB05.

The comparison makes use of the dense rain gauge network deployed in the metropolitan Baltimore area as part of the Baltimore Ecosystem Study, the IFLOWS gauge network, and a disdrometer located at the University of Maryland Baltimore County campus approximately 20 km from TBWI.

The study results may be summarized by noting that very good agreement was often obtained between TDWR reflectivity and disdrometer-based reflectivity, particularly when only minimal rain intervened between the radar and the observation point. This is an effect of the high spatial and temporal resolution of the TDWR data, as well as its proximity to the disdrometer. Since the TDWR estimates also showed more spatial detail than did the WSR-88D estimates, we are confident that these details are realistic and that the enhanced spatial resolution is effective in better detection of areal-average rainfall over small basins.

Under the agreement, OHD maintains a routine archive of TDWR base reflectivity products prepared in real time by a prototype Supplemental Product Generator operated by the NWS/OS&T. Samples of this data for several rain events during the summer and early autumn of 2004 were forward to Princeton for derivation of rainfall estimates, testing of an attenuation correction method, and subsequent comparison with WSR-88D estimates.

Initial results were based on observations during the thunderstorm events of 7 July and 4 August 2004, which produced heavy rainfall over Baltimore. The 7 July event (Fig. 2-1) yielded rainfall in excess of 100 mm in less than 3 hours and produced the flood of record near the outlet of Dead Run in the northwestern part of the city (personal

communication from James Smith). A comparison of time series of TDWR reflectivity with disdrometer reflectivity during this storm appears in Fig. 2-2. The disdrometer trace (marked with crosses) and TDWR trace (marked with circles) are very close for the two-hour period 1830-2045 UTC, including some intervals with reflectivity as high as 50 dBZ. After 2100 UTC, the TDWR began to underestimate as heavy precipitation came between the radar and disdrometer. .

In further work, an attenuation correction algorithm was implemented for the TDWR reflectivity observations. The algorithm employed a specific attenuation coefficient in power law form:

$$K_r = aR^b$$

where K_r is the one-way specific attenuation in dB km^{-1} and R is the rainfall rate in mm h^{-1}. The rainrate is accumulated over the intervening space between the radar and the point in question. In this study, values of 1.0 and 0.01 were used for *a* and *b* respectively. A time series of reflectivity from the disdrometer and from TDWR with and without this attenuation correction, for an 18-minute period of heavy rainfall on 4 August 2004, appears in Fig. 2-3; in general the disdrometer values fell between the adjusted and unadjusted TDWR estimates.

During the course of the study, there were several instances in which the WSR-88D and TDWR produced estimates of basin-average rainfall that differed substantially in amount and/or timing. As shown in Fig. 2-4, from 13 August , the peak rainrate could differ by a factor of 2 (15 vs. 30 mm h^{-1}); Fig. 2-5 shows instances on 11 and 13 August in which the TDWR indicated rainrate peaks approximately 15 minutes before the WSR-88D did.

We note that it can be difficult to differentiate among the effects from different spatial and temporal resolutions and range effects. However, the WSR-88D does fully resolve the Dead Run sub-basins, though of course with fewer data points than does the TDWR. The results shown in SB05 indicate that enhanced spatial resolution of WSR-88D estimates would increase their accuracy. Further increases in utility would be realized if the temporal resolution of the WSR-88D could be increased as well.

Reference

Smith, J. A., and M. L. Baeck, 2005: An assessment of TDWR rainfall esimtates for flash flood forecasting. Report to the Office of Hydrologic Development, 36 pp. [Included in MOU Final Report Package].

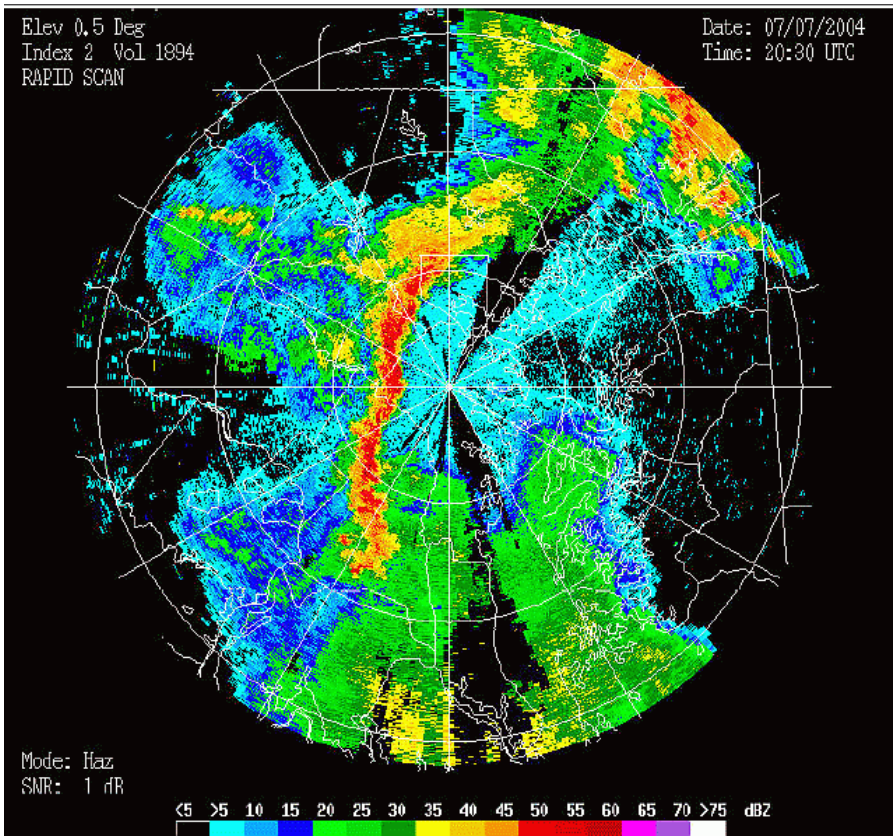

Figure 2-1. Reflectivity from the BWI airport TDWR unit at 2030 UTC, 7 July 2004.

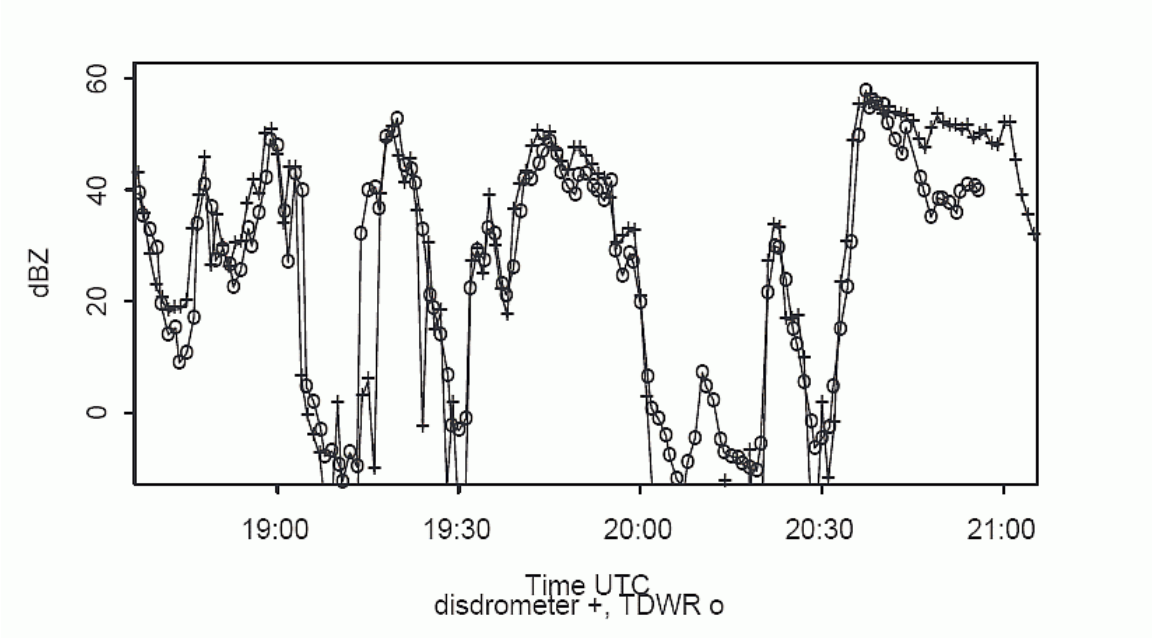

Figure 2-2. Trace of disdrometer (+) and TDWR (o) reflectivity estimates over northwestern Baltimore during the 7 July 2004 storm event, from SB05.

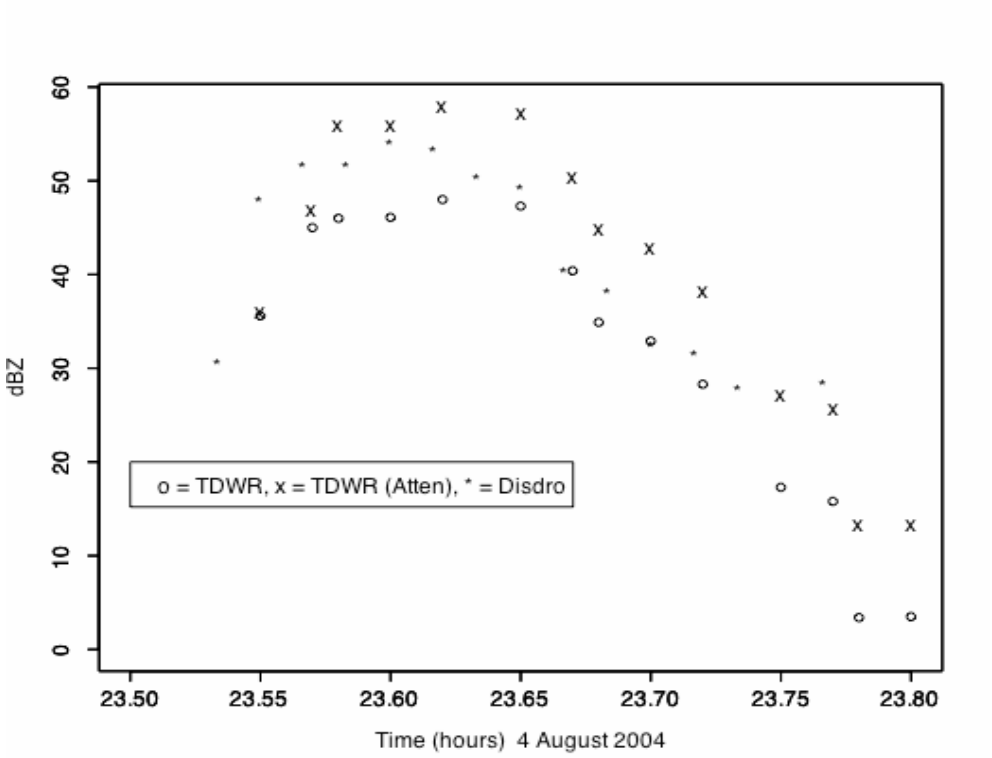

Figure 2-3. Instantaneous reflectivity values from the 4 August 2004 storm based on disdrometer (*), TDWR (°) and TDWR with attenuation correction (X), from SB05.

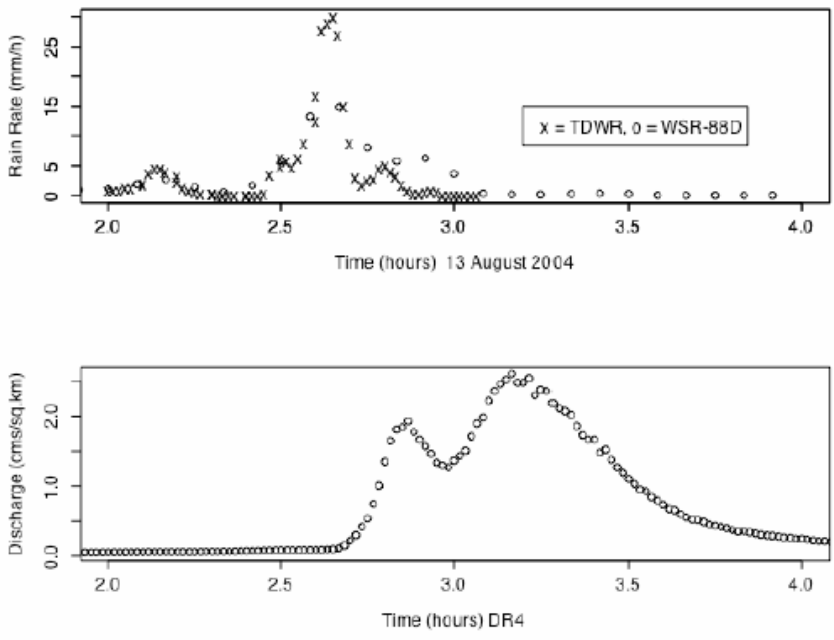

Figure 2-4. Basin-average rainfall rate and outlet discharge for Dead Run sub-basin "DR4" on 13 August 2004. TDWR values are indicated by "X" and WSR-88D by "o". Note that highest rainrate for WSR-88D was 15 mm h^{-1}, but 30 mm h^{-1} from TDWR.

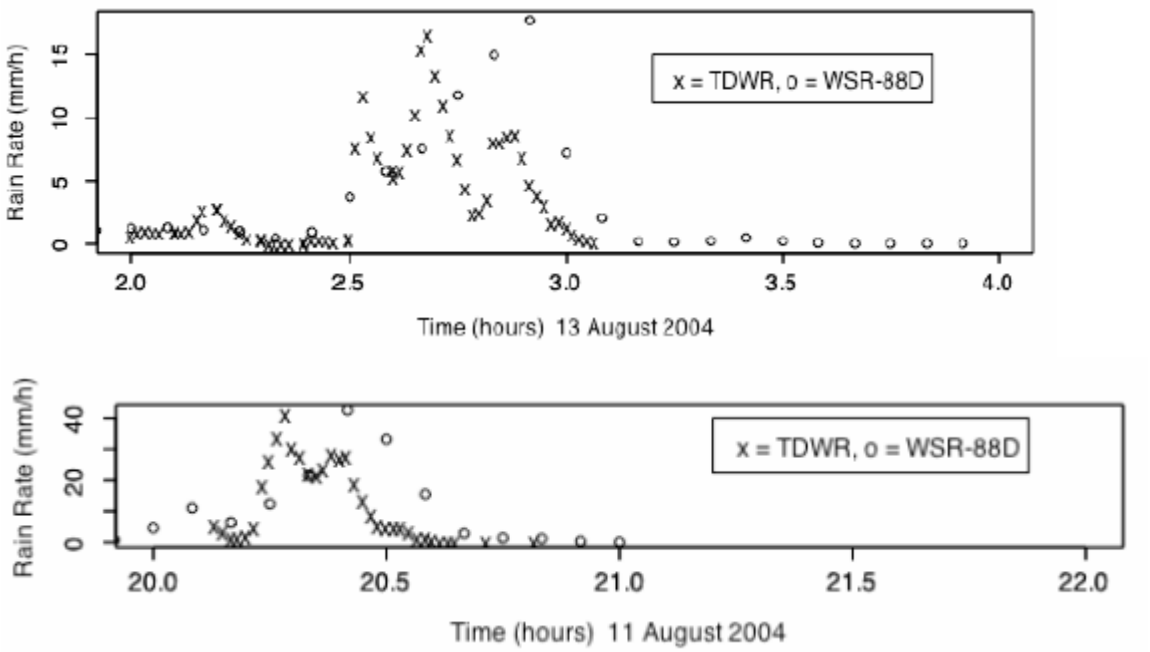

Figure 2-5. Basin-average rainfall rainrate for sub-basin "DR3" on 13 August 2004, and subbasin "DR4" on 11 August 2004, from SB05. In both events the TDWR indicated the rainfall peak about 15 minutes in advance of the WSR-88D.

Task 3: Radar-Based Probabilistic Quantatitive Precipitation Estimates (PQPE)

3.1 Formulation of the radar rainfall error model

A project to develop radar-based PQPE has been supported by ROC and the Advance Hydrologic Prediction Service (AHPS) program for several years. We continue to work with contractors at the University of Iowa (principal investigator Witold Krajewski) to deliver an algorithm capable of outputting radar rainfall estimates in probabilistic form.

Work at Iowa now focuses on development of the algorithm in a form that is useable within the ORPG environment. An initial report on the algorithm documentation (Krajewski and Ciach 2005) was delivered to OHD in June 2005.

Within OHD, we are evaluating the basic results on the statistical properties of radar rainfall estimates that have been presented by the Iowa contractors, and are developing a simple model for the error characteristics of the Digital Precipitation Array (DPA) 1-h rainfall product. The DPA is used extensively in the Multisensor Precipitation Estimation (MPE) package in AWIPS. This analysis can be extended to generating probabilistic products, as will be shown below.

As reported by Krajewski and Ciach (2005, or KC05), horizontal-polarization rainfall estimates based on a Z-R relationship show some recurring error characteristics when compared with rain gauge observations. In data samples where both the radar and gauge indicate measurable rainfall, and the estimates are collected into amount categories based on the radar estimates, the radar values are biased low for small rain amounts (< 0.1 in h^{-1}), and are biased high for larger amounts (> 0.2 in h^{-1}). The bias effects generally become smaller (bias tends toward 1) as the accumulation period increases.

In Fig. 3-1, characteristic rainrate-dependent biases are shown for KTLX rainfall estimates relative to Agricultural Research Service (ARS) Micronet rain gauges in the Little Washita basin in central Oklahoma. The abscissa is rainfall amount, the ordinate the expected (mean) gauge value. The bias is generally near one up to a certain rainfall magnitude, which itself grows larger as accumulation period increases. Long-term biases (0.8 to 0.95 depending on the season) were removed prior to this analysis.

We were able to substantially duplicate this result with data from several other radar umbrellas, considering data from the warm season May-September 2004. As shown in Fig. 3-2, a similar behavior is noted for 3 widely-separated radar umbrellas, with varying bias characteristics. Differences between the traces in Figs. 3-1 and 3-2 are due partly to the type of data sample (Fig. 3-1 includes all gauge values for radar values > 0; Fig. 3-2 includes only cases where both radar and gauge were > 0), and partly because the traces were extended to higher values in Fig. 3-1.

The standard deviation of the radar/gauge multiplicative error appears to have a characteristic distribution, as well. As shown in Fig. 3-3, from KC05, the value is large at small rainrates and tends toward a value of 0.5 for rainrates above about 25 mm for all accumulation periods.

Note that, given the mean and standard deviation of the multiplicative error as a function of the radar estimate itself, it is possible to estimate the probability of any rain gauge observation, given the radar estimate. As shown in Fig. 3-4 from KC05, the distribution of the multiplicative error closely approximates a Gaussian distribution, from which probabilities of any given amount can be calculated from standard formulae.

The authors of KC05 propose that the entire error distribution for any one accumulation period can be approximated by one simple power-law function of rainfall rate for the bias (fitting a curve in Fig. 3-1), and another for the magnitude of the standard deviation (fitting a curve in Fig. 3-3). Range dependence might be incorporated by a simple adjustment. Thus it appears that the error distribution for rainfall estimates can be adequately described by 4-6 parameters, which could easily be included with the rainfall product.

3.2 Statistical adjustments to 1-h rainfall estimates

As is apparent in Figs. 3-1 and 3-2, the bias at higher rainfall amounts might contribute substantially to systematic error. To test this possibility, we derived a quadratic function fit to the points for KTLX in Fig. 3-2, and applied this as a correction to gauge/radar pairs in the KFFC sample. The correction has little influence on rainfall amounts < 0.1 inch, but for higher amounts results in a substantial adjustment toward lower values. We found that for all cases in which the original DPA value was ≥ 0.25 inch, the RMS error was reduced by the adjustment. For the original DPA values the RMS error was 0.35 inch, while for DPA with long-term bias adjustment (multiplying all values by 0.93) the RMS error was 0.33 inch. However, applying both the long-term bias and the statistical rainrate-dependent adjustment reduced the RMS error within that subsample to 0.31 inch.

3.3 Sample probabilistic radar rainfall products

To demonstrate two types of probabilistic products in a straightforward manner, we further evaluated the gauge value function shown in Fig. 3-2, and derived curves for the probability of fixed 1-h amounts (0.1 in or 2.5 mm and 0.5 in or 12.5 mm), and rain amount corresponding to a fixed probability of exceedance (here, 25% and 50%). In practice, these functions could be derived from power-law functions and a knowledge of the Gaussian distribution, as noted in 3.1 above.

The sites evaluated were TLX (Twin Lakes OK), INX (Tulsa, OK), MPX (Minneapolis, MN), MLB (Melbourne FL), and LWX (Sterling VA). Data were collected during the period May-September 2004. The number of available gauge/radar pairs ranged from 14,500 at MPX to over 20,000 at the other sites. Long-term MFB values ranged from 0.80 at TLX to 1.05 at LWX. At this stage no attempt has been made to insure a common Z-R relationship over time or among sites, but most employed the warm-season convective relationship $Z=300R^{1.6}$ during the period. No attempt has been made to account for range effects. All data pairs were collected within the effective coverage area as determined from DPA coverage masks used within AWIPS MPE.

It is apparent from the probability curves for 0.1 and 0.5 in (Figs. 3-5 and 3-6) that the larger radar-estimated amounts are biased high relative to point gauge observations. While the MFB-adjusted radar estimates and gauge observations have the same mean, the

bias calculation must necessarily be weighted toward correcting the radar at the lower end of the amount distribution, where the majority of the observations fall. This leads to radar overestimation at the higher ends of the distributions.

Therefore for 1-h amounts greater than about 0.1 in, the average point gauge amount is lower than the average radar value. For the P(0.1") distribution (Fig. 3-5) the curves are very similar for radar estimates up to about 0.3 in, and they cluster around 0.9 (90% probability) for values greater than 0.6 in. For the P(0.5") distribution (Fig. 3-6) there is greater spread in the curves, as might be expected given that only about 5% of the cases feature gauge observations ≥ 0.5 in. The curves do tend to converge for radar rainfall of at least 0.9 in.

A related probabilistic quantity is the rain amount corresponding to the 75th percentile of the distribution of all amounts. This also corresponds to the amount that has a 25% chance of being exceeded at any one point, is shown in Fig. 3-7. This might be considered a "reasonable threat" rain amount in terms of public perception, by analogy with current NWS practice of entering a mention of rainfall in text forecasts whenever the probability of precipitation exceeds 20% or 30%. Over much of the range of radar-estimated values, the 25th percentile rainfall is near or slightly greater than the rainfall estimate, consistent with the fact that the expected (mean) rainfall is consistently less than the radar estimate over much of the range of the distribution.

The median point rain amount (50th percentile amount) as a function of the radar DPA value is shown in Fig. 3-8. For any small range of DPA values, this is the point amount that will be exceeded half the time and not exceeded half the time (note that the mean point amount is generally larger than the median because the distribution is skewed towards higher amounts).

Application of this information involves output or display of the probability or the percentile amount values from the points on the curves corresponding to a given DPA amount. A bias-adjusted 1-h radar precipitation mosaic, and corresponding probabilistic products, are shown in Fig. 3-9. The 1-h rainfall for 1200 UTC on 19 June 2004 is shown in (a), with some locally heavy amounts in excess of 1 inch indicated over south-central Oklahoma. The corresponding 50th percentile amounts (based on the curve in Fig. 3-8) are shown in (b). For lighter amounts (less than about 0.2 inches indicated in the DPA), there is little apparent difference. The effects of overestimation in the higher portion of the radar rainfall distribution are apparent, however, since the extent of the 1-inch area (coded bright green and yellow) is noticeably smaller. Probability of 0.5 inch, based on the curves in Fig. 3-6, appears in (c). Some values in excess of 50% appear in the areas with DPA rainfall near 1 inch.

Again, we emphasize that the probability and percentile curves shown here are specific to 1-h accumulations, in the warm season. Substantially different bias characteristics can be expected for longer accumulation periods, or cool-season rainfall.

3.4 Methods of operational dissemination of PQPE information

Obviously, there are many potential probabilistic applications, so many that it would be difficult to accommodate more than a few as additional ORPG products. This situation

suggests a simpler approach, namely disseminating only the basic information on the error distribution. End users would derive the particular probabilistic quantities they need by interpreting the distribution properties.

As noted by KC05 and in 3.1 above, it appears that the distribution of ground truth precipitation values about any given radar estimate can be described by a small set of parameters. For any one radar site during a given season, and for a given accumulation period, the parameters are: the long-term bias (already disseminated along with QPE products in the bias table), two parameters to describe the rainrate-dependent bias curves as shown in Fig. 3-1, and two parameters to describe the standard deviation of the values as a function of rainrate, as shown in Fig. 3-3. It is possible that an additional parameter to describe range effects may be desirable. The long-term mean field bias for any one radar is already maintained by routine radar and rain gauge processing within AWIPS and forwarded to the ORPG. The remaining parameters could be estimated within AWIPS or centrally, from DPA products and rain gauge data.

The parameters could be included in the Supplemental Precipitation Data (SPD) product, or appended as text along with other data in the DPA. External user documentation or an external algorithm would be required to describe the application of the parameters to a variety of probabilistic products.

References

Krajewski, W. F., and G. J.Ciach, 2005: Towards Probabilistic Quantitative Precipitation WSR-88D Algorithms: Data Analysis and Development of Ensemble Model Generator: Phase 4. Report to Office of Hydrologic Development under NOAA Contract DG133W-02-CN-0089, 69 pp. [Included in final MOU report package].

Krajewski, W. F., G. J.Ciach, and K. P. Georgakakos, 2004: Final Report: Towards Probabilistic Quantitative Precipitation WSR-88D Algorithms: Preliminary Studies and Problem Formulation, Phase 3. Report to Office of Hydrologic Development, 24. pp. [Included in final MOU report package].

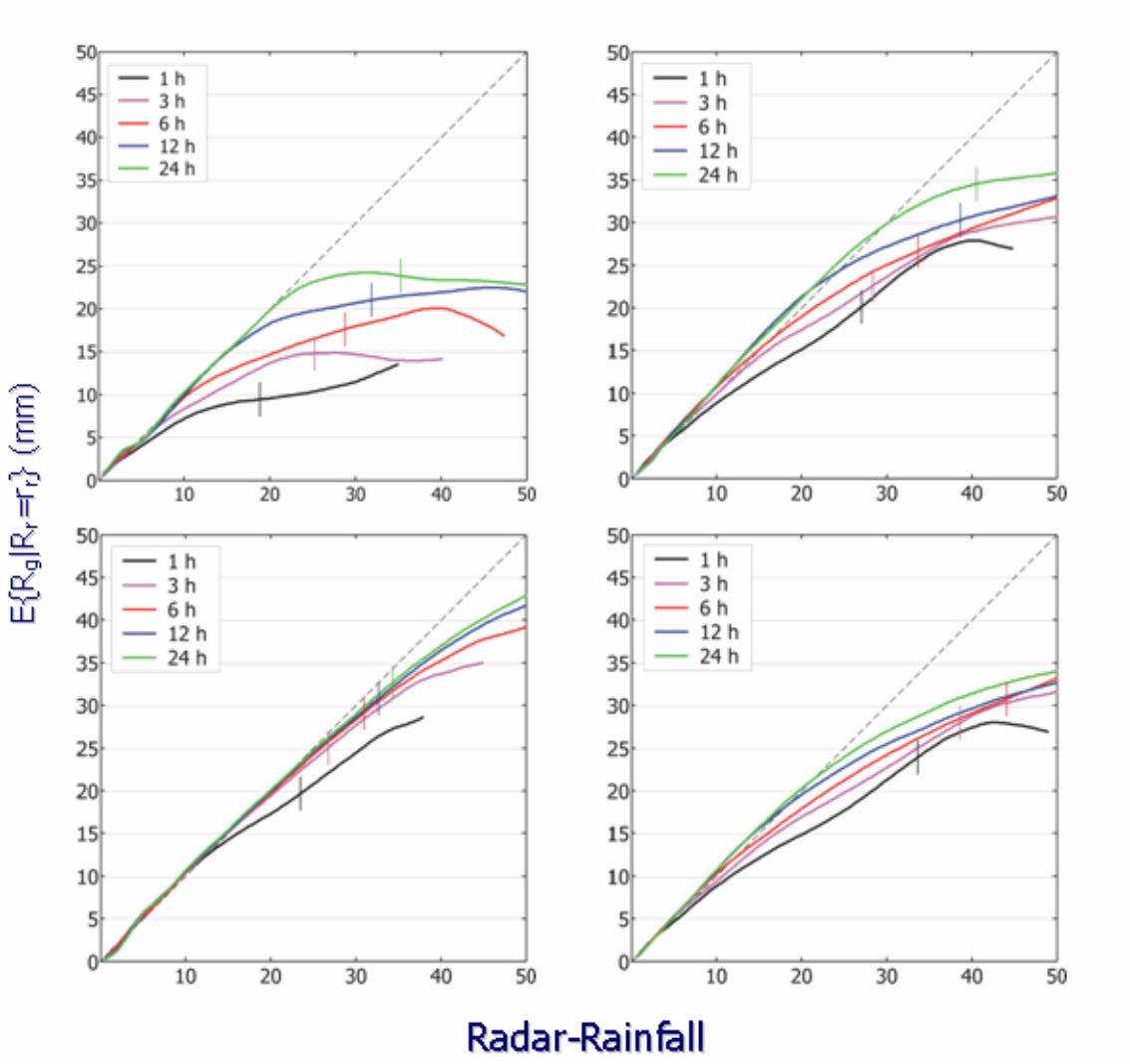

Figure 3-1. Expected rain gauge value as a function of radar rainfall (mm) for different seasons and accumulation periods, KTLX umbrella, 1997-2003. From KC05.

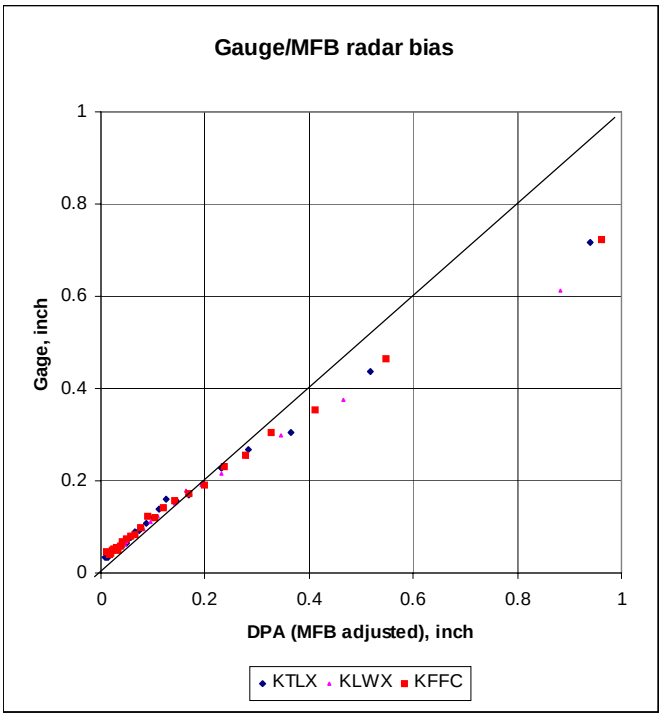

KTLX bias: 0.7
KLWX bias: 1.07
KFFC bias: 0.93

Figure 3-2. As in Fig. 3-1, except for 1-h radar/gauge estimates throughout the WSR-88D umbrellas KTLX, KLWX, KFFC, May-September 2004. Long-term biases for each umbrella are as shown.

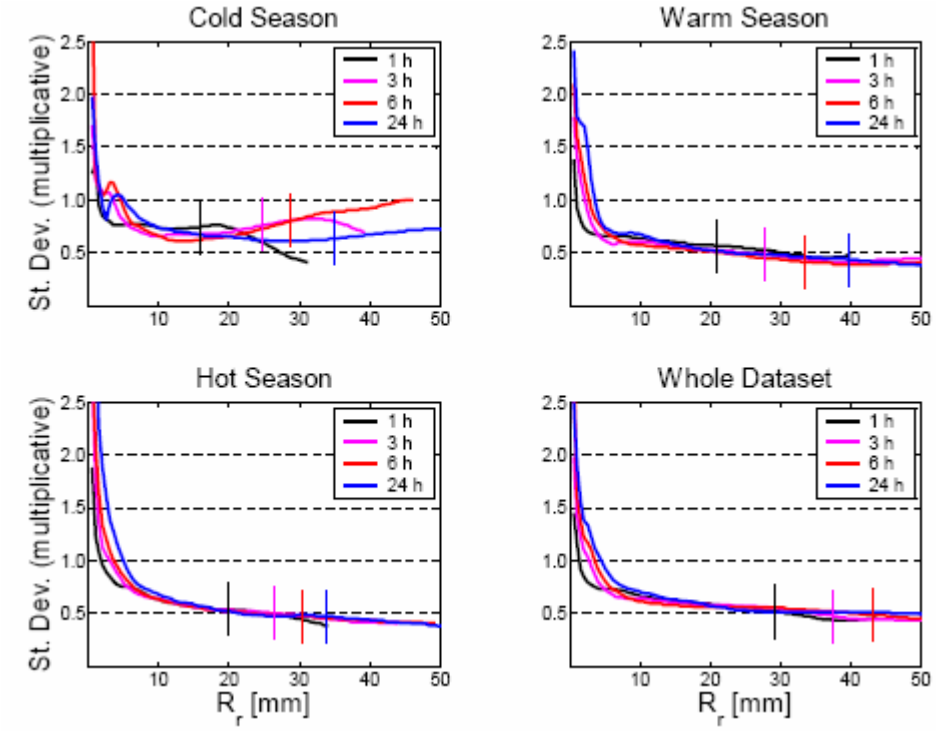

Figure 3-3. Standard deviation as a radar/gauge multiplicative error as a function of radar rainrate, same data sample as in Fig. 3-1. From KC05.

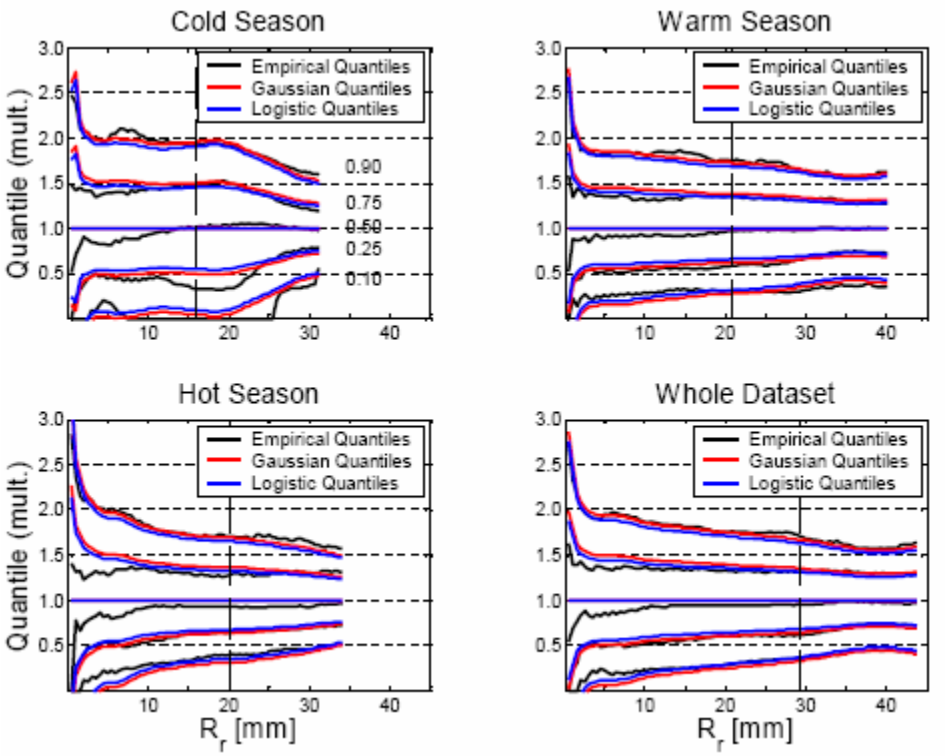

Figure 3-4. Modeled and observed quantiles for the distribution of the multiplicative errors corresponding to the data sample in Fig. 3-1. From KC05.

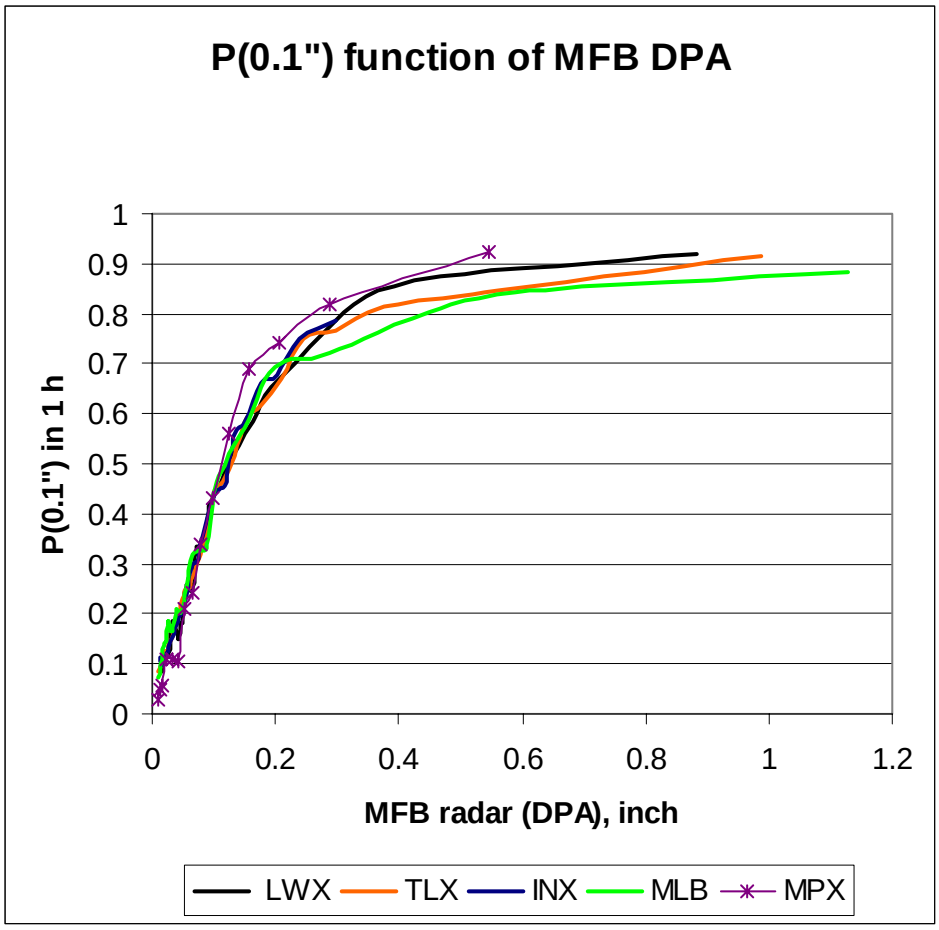

Figure 3-5. Probability that gauge rainfall at a given point will exceed 0.1 inch in 1 h, as a function of mean field bias-adjusted DPA value.

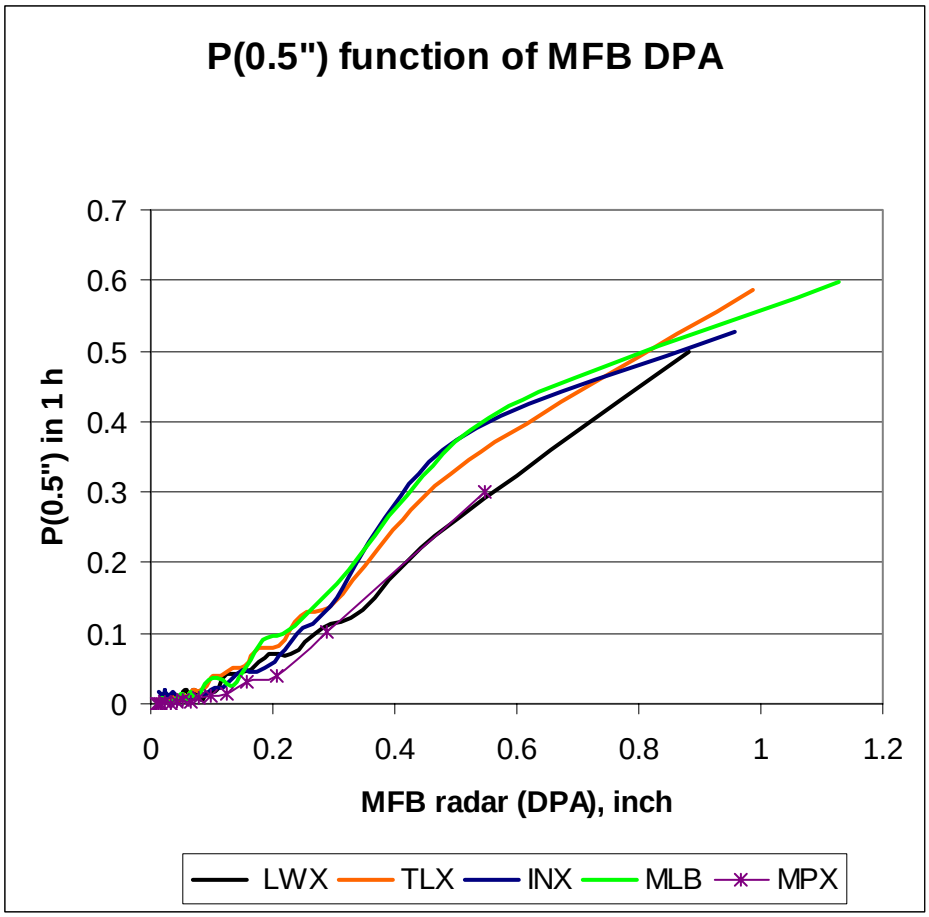

Figure 3-6. As in Fig. 3-1, except probability of 0.5 in rainfall.

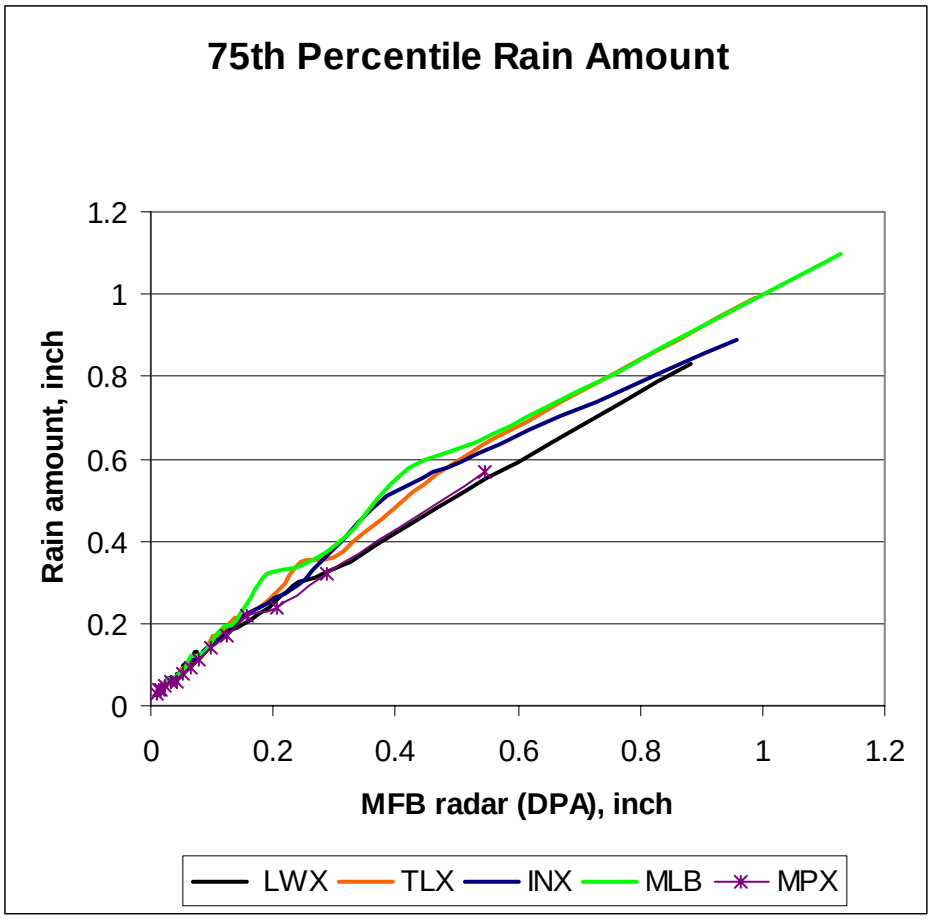

Figure 3-7. 1-h rainfall corresponding to 75th percentile of amount distribution (i.e. 25% of observed point values exceed this amount).

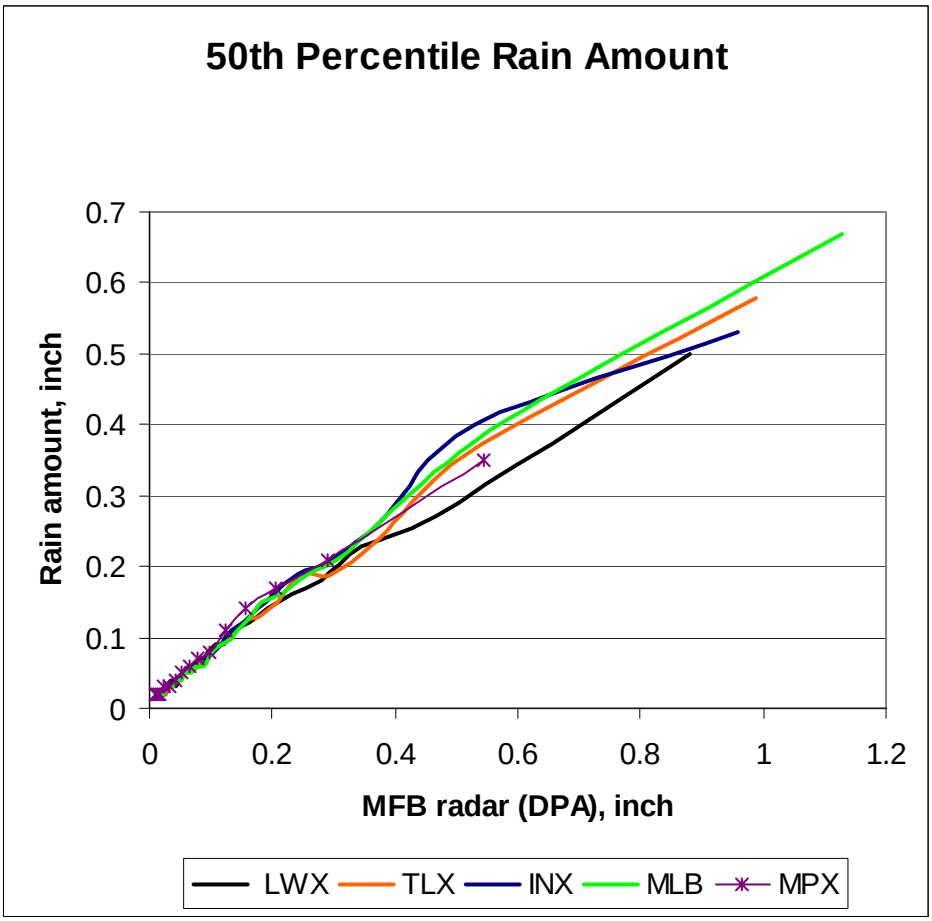

Figure 3-8. 1-h point rainfall corresponding to 50th percentile of amount distribution (i.e. 50% of observed point values exceed this amount).

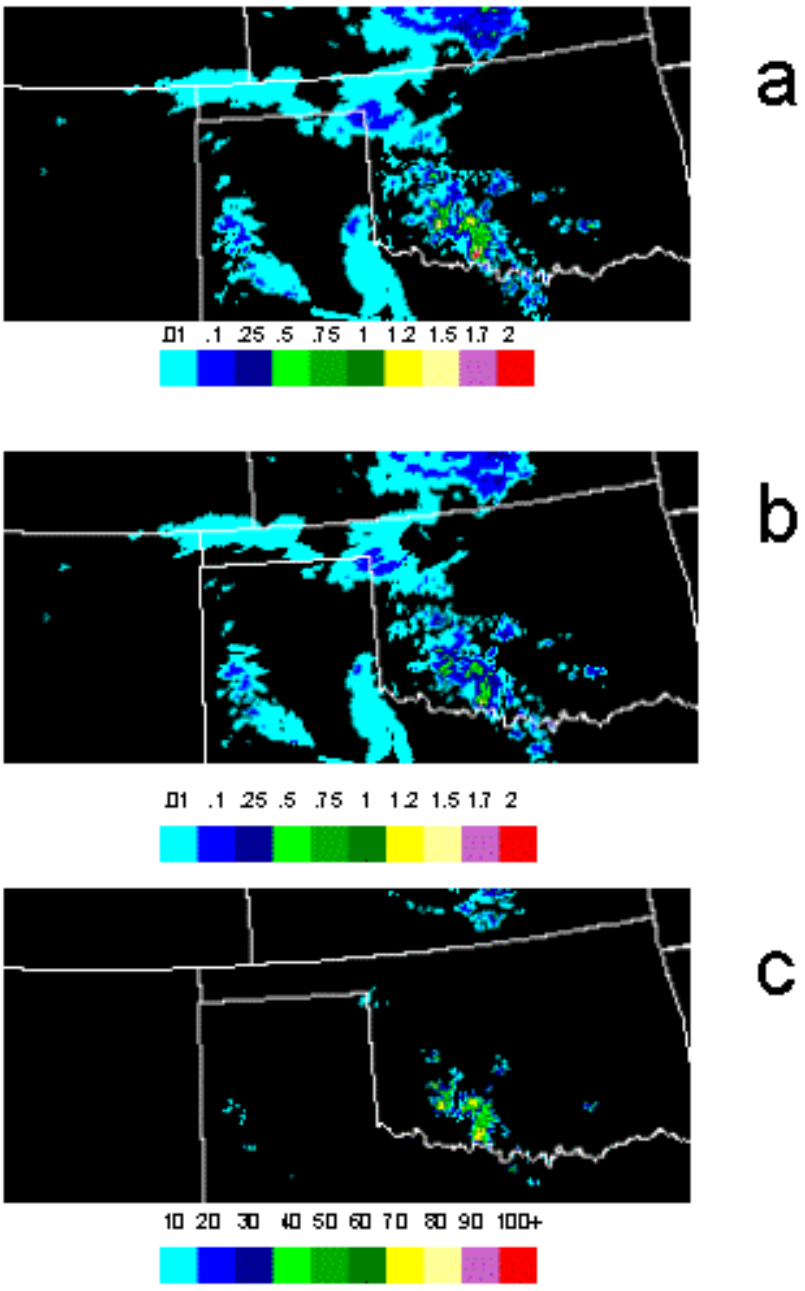

Figure 3-9. Radar 1-h precipitation estimates valid 1200 UTC 19 June 2004 (a), corresponding 50th percentile rainfall amount (b), and corresponding probability that point rainfall exceeded 0.5 inch (12.5 mm). Amounts in (a) and (b) are in inches, in (c), per cent.

Task 4: Assessment of 2004-2005 Dual-Polarization Radar Rainfall Estimates

4.1 Analysis of KOUN dual-polarization and WSR-88D horizontal polarization rainfall estimates, spring 2005

Ryzhkov et al. (2004) have documented significant improvements in rainfall estimation that could be achieved through the implementation of dual-polarization technology. Their recent published comparisons to date have relied primarily on comparisons between horizontal-polarization Z-R estimates and multi-parameter dual-polarization estimates from the same experimental radar unit in Norman, Oklahoma (KOUN). We wished to extend the assessment to a comparison between the experimental dual-polarization estimates and coincident operational horizontal-polarization estimates from the WSR-88D unit at Twin Lakes, Oklahoma (KTLX). The Digital Precipitation Array (DPA) products from KTLX are used in operational precipitation analyses for hydrologic forecasting.

In this analysis, data from 51 hours during the period May-June 2004, provided by NSSL, were considered. There was considerable convective rainfall in some of the cases. One-hour accumulations with nominal ending times between :58 minutes and :02 minutes during the hour were collated with rain gauge reports ending within the same 5-minute time window. Of the variety of multi-parameter dual-polarization algorithms provided by NSSL, we selected the "synthetic" algorithm output, which features an optimal combination of Z, Z_{DR}, and K_{DP} algorithm output. The operational DPA product without mean-field bias (MFB) correction represented WSR-88D estimates. Though the MFB correction would improve some of the verification statistics, the wide range in gauge network density across the conterminous U.S. causes the correction to be problematic in some areas. Some of our comparative verification statistics are insensitive to bias. Because the original dual-polarization estimates were presented on a 2-km Cartesian grid, while the DPA products have a nominal grid spacing of 4 km, we considered both the original dual-pol values and a local 2x2 box average.

A total of 4952 gauge/radar observation pairs that were common to both radar units were collected from the set of approximately 6200 available. Though the units are fairly close, their effective coverage areas do not overlap completely, and some of the periods covered by dual-polarization measurements were missing from our archive of DPA's. All available pairs were considered, including those in which both radar and gauge indicated < 0.01 inch.

The radar estimates were verified in terms of RMS error, nonlinear correlation (correlation ratio), and rank correlation. The correlation ratio is a statistic which indicates the percentage of predictand variance (in this case that of the gauge values) is explained by a predictor regardless of the nature of the relationship between the two, which is often nonlinear and sometimes not monotonic (Panofsky and Brier 1968). For situations in which the predictor/predictand relationship is approximately linear, the correlation ratio approaches the square of the linear correlation coefficient.

Summary statistics on the gauge and radar estimates appear in Fig. 4-1. About 10.4% of the gauges estimates were ≥ 0.01 in, compared to 12.1% and 12.6% for the 2-km and 4-

km dual-pol estimates, respectively, and 14.4% for the DPA estimates. The average 1-h rainfall was 0.0119 in for the gauges, 0.0148 and 0.0144 in for the 2-km and 4-km dual-pol estimates, and 0.0195 in fro the DPA's.

We found that within the dataset as a whole, the synthetic dual-polarization estimates improved on the DPA estimates in terms of correlation ratio and RMS error (see Fig. 4-2). The 2-km estimates explained 0.41 of the predictand variance, while the DPA estimates explained 0.38. The synthetic estimates averaged to 4 km explained 0.44 of the variance; this is likely due to the effect that horizontal smoothing has in reducing small-scale variability in the radar estimates that is not reflected in the point gauge observations. Likewise, the dual-polarization estimates featured smaller RMS errors than the DPA estimates.

Of similar interest is the verification within the set of 860 cases in which at least one of the observation sets indicated measurable precipitation ($\geq$ 0.01 in). Here, the dual-pol estimates were also superior to the DPA, with correlation ratios of 0.32 and 0.36, compared to 0.30 for the DPA estimates. The RMS errors were also lower for the dual-polarization estimates (Fig. 4-3).

In terms of detection of measurable precipitation (both radar estimate and gauge amount $\geq$ 0.01 in), the three sets of estimates were very similar, being correct 93% of the time for the dual-pol estimates and 92% of the time for the DPA estimates.

4.2 Analysis of dual-polarization rainfall estimates, Spring 2005

Data from some 2004 cases were reprocessed by NSSL to incorporate new radar calibration checks, and these have been combined with data from the period March-June 2005 to form a larger data sample, which is still under analysis. The sample currently amounts to approximately 115 discrete hours with some precipitation. The analysis described above will be repeated on this larger sample, as outlined in the FY 2005 MOU.

As shown in Fig. 4-1, it appears that all the 1-h radar estimates are biased high relative to gauge values in terms of both coverage of precipitation and amounts. An initial statistical analysis has been carried out to determine the degree to which the dual-polarization estimates are affect by rainrate-dependent bias (as described under Task 3). There are some apparent differences between the horizontal- and dual-polarization estimates for amounts > .1 inch h^{-1} (2.5 mm h^{-1}), as shown in Fig. 4.4, which contains images for 3 different estimates of 1-h rainfall ending 1000 UTC, 13 May 2005. Fig. 4-4a,b show dual-pol "synthetic" and standard Z_h estimates from the KOUN unit, while Fig. 4-4c shows estimates from the DPA product from the KTLX unit. There is substantial resemblance between the DPA and Z_h fields, though it appears that the KTLX DPA has some higher rainfall amounts above 0.25 inch north and northeast of the radar. However, the area of rain > 0.1 inch is substantially smaller in the synthetic product (Fig. 4-4a).

An alternative analysis based on percentiles was undertaken. Rainfall values for the 70^{th}-99^{th} percentiles of the radar amount distributions are shown as functions of the rain gauge percentiles in Fig. 4-5. These data are from a set of 6228 radar-gauge pairs from 2005 and reprocessed 2004 data. In this analysis, gauge and radar values are not treated as

physically collocated entities, but only as members of a distribution from common times and locations.

The last datum is the 99th-percentile amount. For example, the figure shows that the 95th percentile amount for the rain gauge distribution is 0.15 inch, while the 95th percentile amount for all three radar estimates is approximately 0.25 inch. For the 70th through the 94th percentiles, the DPA values are larger than the dual-polarization estimates (consistent with Fig. 4-4), while the DPA percentiles are lower at the very top of the distribution. This suggests that the dual-pol estimates are still biased high relative to gauge amounts (as are the operational DPA values).

Further analyses for RMS error, range- and magnitude-dependent biases, and multi-hour time periods will be carried out on the expanded 2004-2005 data sample. The analysis will include additional rain gauge data from the Oklahoma Mesonet, which has recently been acquired in archived form.

References

Panofsky, H. A., and G. W. Brier, 1968: *Some Applications of Statistics to Meteorology.* Pennsylvania State University Press, University Park, 224 pp.

Ryzhkov, A. V., T. J. Schuur, D. W. Burgess, P. L. Heinselman, S. E. Giangrande, and D. S. Zrnic, 2004: The Joint Polarization Experiment: Polarimetric rainfall measurements and hydrometeor classification. Submitted to *Bull. Amer. Meteor. Soc.*

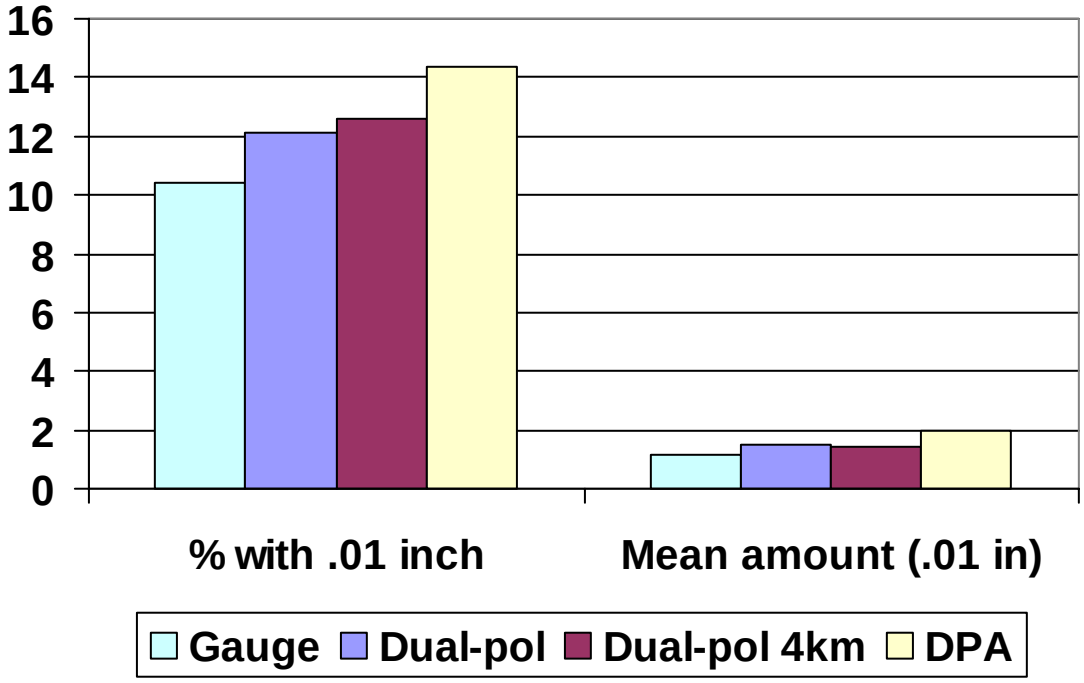

Figure 4-1. Summary statistics for the 4592 1-h rainfall estimates and gauge reports evaluated.

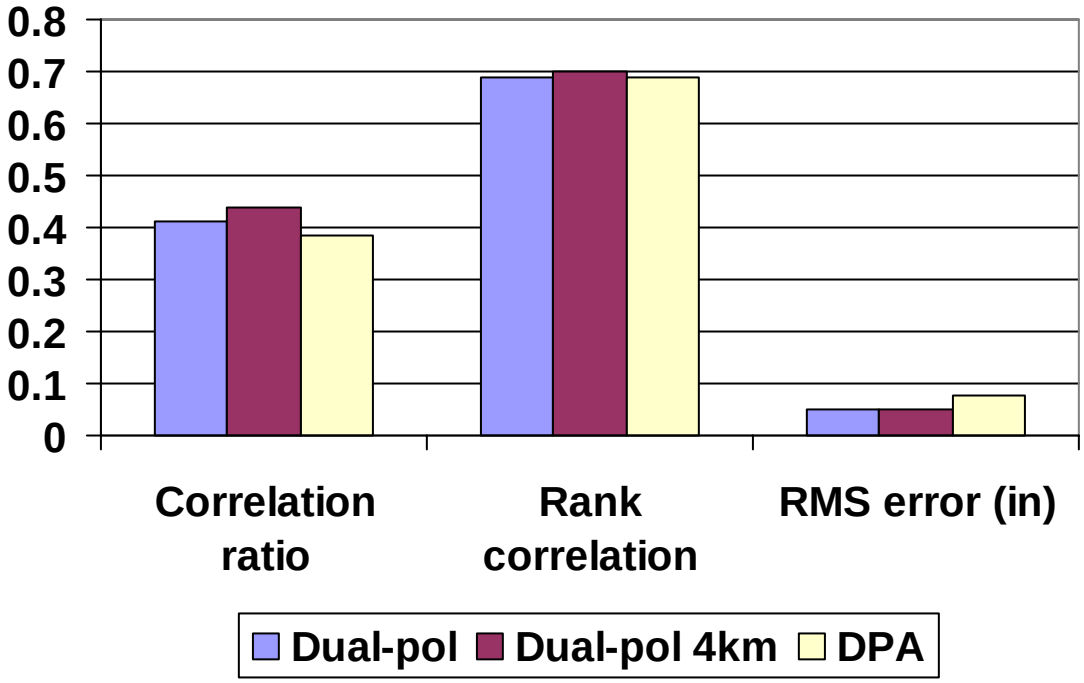

Figure 4-2. Verification scores for Synthetic dual-polarization algorithm, synthetic algorithm smoothed to 4-km resolution, and WSR-88D Digital Precipitation Array product. Verification is for 1-h rain gauge amounts, 4592 cases, May-June 2004.

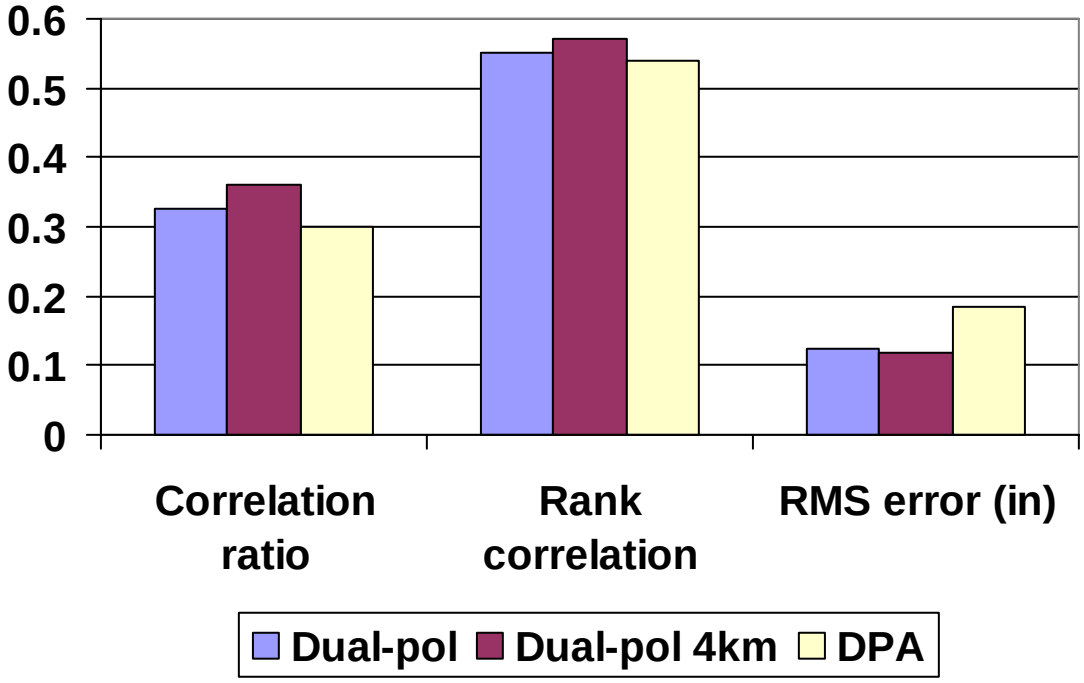

Figure 4-3. As in Fig. 4-2, except for 860 cases in which at least one sensor system indicated rainfall ≥ 0.01 inch.

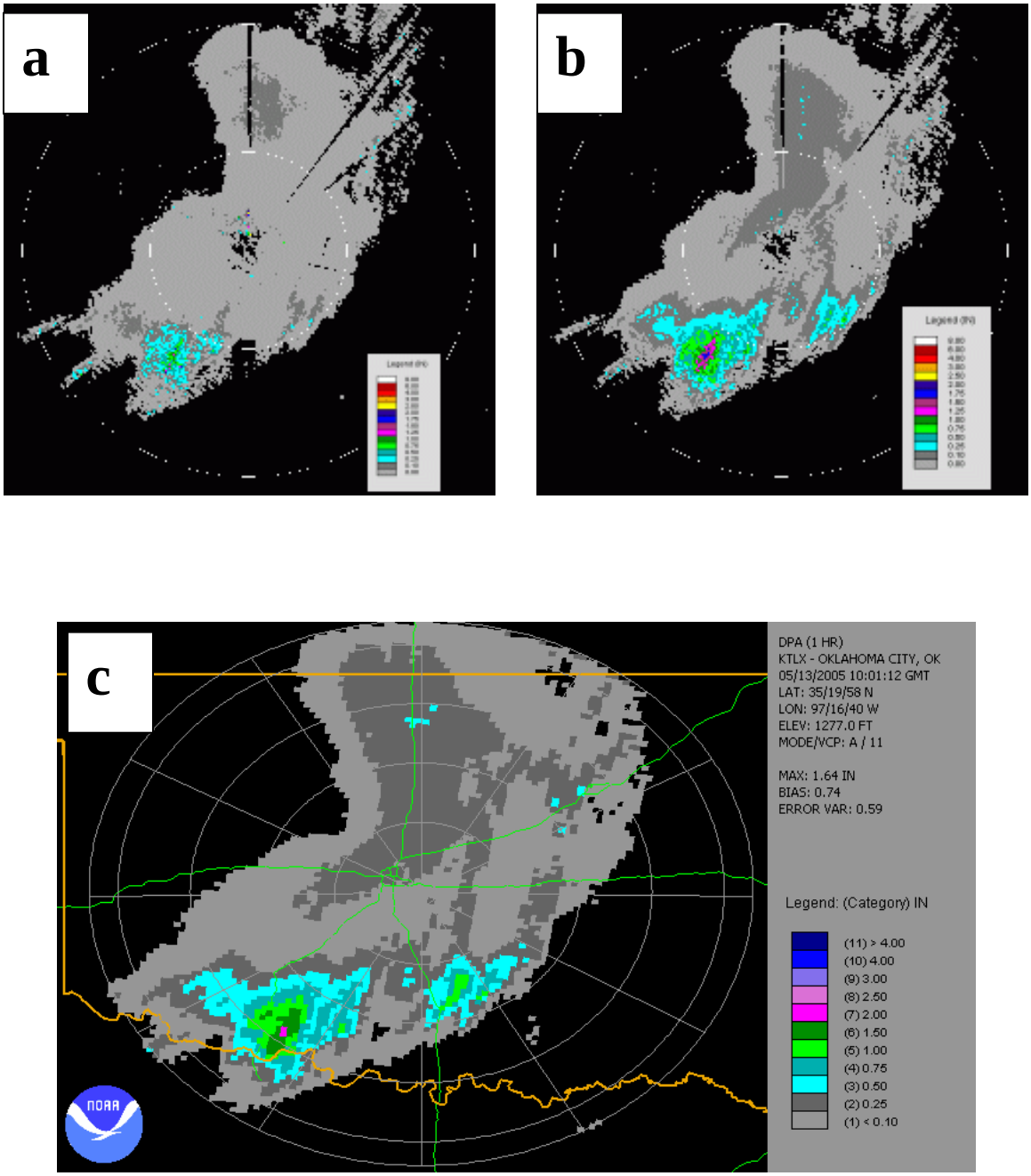

Figure 4-4. One-hour precipitation ending 1000 UTC 13 May 2005, from (a) KOUN dual-pol Synthetic algorithm; (b) KOUN Z_h algorithm; (c) KTLX DPA product.

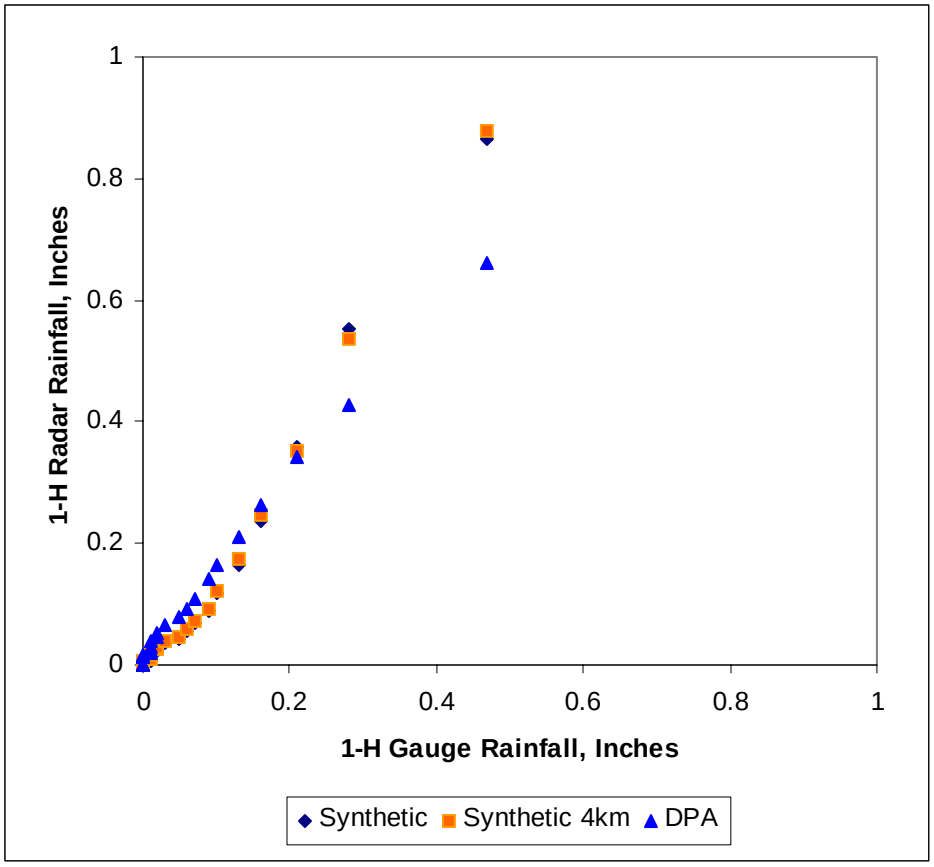

Figure 4-5. Rainfall values corresponding to 70th-99th percentiles of distribution of 6228 radar/gauge pairs in the KOUN/KTLX umbrella, May-June 2004-2005. All values below 70th percentile are zero. Each point in the traces corresponds to a 1% increment (62 individual cases). Note that the distribution for all radar estimates is higher than gauge amounts for values > 0.1 inch in one hour.